

Changing the Electronic Spectrum of a Quantum Dot by Adding Electrons

S. R. Patel, D. R. Stewart, and C. M. Marcus

Department of Physics, Stanford University, Stanford, California 94305

M. Gökçedağ, Y. Alhassid, and A. D. Stone

Center for Theoretical Physics, Sloane Physics Laboratory, Yale University, New Haven, CT 06520

C. I. Duruöz and J. S. Harris, Jr.

Electrical Engineering Department, Stanford University, Stanford, California 94305

(May 16, 2018)

The temperature dependence of Coulomb blockade peak height correlation is used to investigate how adding electrons to a quantum dot alters or “scrambles” its electronic spectrum. Deviations from finite-temperature random matrix theory with an unchanging spectrum indicate spectral scrambling after a small number of electrons are added. Enhanced peak-to-peak correlations at low temperature are observed. Peak height statistics show similar behavior in several dot configurations despite significant differences in correlations.

73.23.Hk,05.45.+b,73.20.Dx

Electron transport through irregular quantum dots – i.e. micron-scale islands of confined charge weakly connected to electronic reservoirs – are expected to, and in some cases actually do, exhibit universal statistics associated with quantum chaos [1]. An example where theory and experiment agree well is the distribution of Coulomb blockade (CB) peak heights [2–5]. At temperatures T that are much smaller than the mean level spacing of the dot Δ , transport on a CB peak is mediated by resonant tunneling through a single level [6,7]. Large fluctuations in CB peak heights in this regime reflect the fluctuating strength of coupling of the chaotic wavefunction in the dot to the modes in the leads, leading to universal statistics sensitive only to time-reversal symmetry [2,3], in good agreement with experiment [4,5].

At higher temperatures, $\Delta < k_B T < E_C$, where E_C is the classical charging energy, each CB peak contains contributions from $\sim k_B T / \Delta$ quantum levels, and one would expect roughly this number of adjacent peaks to be correlated in height. This assumes that the spectrum of the dot does not change as electrons are added. On the other hand, if adding electrons alters the spectrum, then the correlation length in peak number, n_c , will not grow beyond a certain value, m , which roughly measures (but is not equivalent to) the number of added electrons needed to completely “scramble” the electronic spectrum.

This Letter presents measurements of the temperature dependence of the CB peak-to-peak height correlation and peak height statistics for gate-confined GaAs quantum dots, and compares these results to finite temperature random matrix theory (RMT) calculations that ne-

glect spectral scrambling [8]. We find that the number of correlated peaks $n_c(T)$ saturates at $m \sim 2 - 5$, with smaller dots saturating at smaller m . At the low temperature end, we find that $n_c(T)$ is *larger* than the value predicted by RMT. That is, correlations in peak heights beyond thermal smearing exist for reasons that are not clear. Some possible explanations are considered below.

In contrast to the dependence on dot configuration found for the peak height correlations (as reflected in $n_c(T)$ and m), peak height *statistics* are found to be very similar for all device configurations. This suggests that peak statistics are more robustly “universal” than peak correlations, not surprising considering that distributions are not sensitive to spectral scrambling. The ratio of the standard deviation to mean of peak heights is found to be smaller than predicted, possibly due to the effects of decoherence.

What does one expect to be the effect of adding electrons on the spectrum of a quantum dot? In the limit of weak electron-electron interactions (and neglecting shape deformations caused by changing gate voltages) a fixed spectrum of single-particle states is simply filled one at a time, leading to $n_c(T) \sim k_B T / \Delta$ and $m \gg 1$. In the opposite limit of strong interactions, the spectrum could be totally scrambled with the addition of each electron, giving $m \sim 1$. For a GaAs quantum dot containing many (~ 100 or more) electrons, RPA calculations [9,10] (appropriate for weak interactions) indicate that fluctuations in the ground state energy due to interactions are small, of order $r_s g^{-1/2} \Delta$ where g is the dimensionless conductance of the dot and r_s is the so-called gas parameter, the ratio of potential to kinetic energy of the electrons ($r_s \sim 1 - 2$ in GaAs heterostructures). For a ballistic-chaotic dot containing \mathcal{N} electrons $g \sim \mathcal{N}^{1/2}$, giving a rough estimate for the number of electrons needed to scramble the spectrum, $1 < m < \sim \mathcal{N}^{1/2} / r_s^2$, assuming that fluctuations accumulate randomly as electrons are added to the dot.

Measurements of CB peak *spacing* statistics have in some cases found rms fluctuations in E_C as large as 15% [11,12], consistent with classical estimates [13] and numerics [11] for strong interactions (where RPA fails), suggesting that one or a few electrons can significantly

alter the charge arrangement of the dot. Other experiments [14] have found smaller fluctuations, of order Δ , suggesting a lesser degree of rearrangement. In all experiments the peak-spacing distribution is found to be roughly Gaussian, which is surprising considering that spin degeneracy would naively imply a bimodal distribution. Suggested explanations include wave-function dependent interactions [9,15] and scrambling due to shape deformation [16]. Magnetofingerprints of CB peaks in dots with $\sim 50 - 100$ electrons show a persistence of both the addition and excitation spectrum over at least 6 peaks, with changes in the excitation spectrum (measured by nonlinear magnetotransport) of order Δ upon adding one electron, leading occasionally to an exchange of a pair of levels in the spectrum [17]. Symmetric, few-electron dots also show a sort of scrambling in the sense that the ground state shell-filling structure may differ from the corresponding excited state before the \mathcal{N}^{th} electron is added, for as few as $\mathcal{N} = 4$ electrons [18]. For such small systems ($\mathcal{N} < \sim 5 - 6$) exact calculations are possible, and a statistical approach to scrambling is not necessary.

Before describing the experiment, we discuss the generalization of the theory of CB peak height fluctuations to temperatures that are comparable or greater than Δ , but without including spectral scrambling [6,8]. Well-formed CB peaks require weak tunneling from each of the levels λ coupling left and right leads to the dot, with tunneling rates $(\Gamma_l^\lambda, \Gamma_r^\lambda) \ll \Delta/h$, and also low bias and temperature, $(eV_{ds}, k_B T) \ll E_C$, where V_{ds} is the voltage bias across the dot. In this regime, the peak conductance G_{max} has the form

$$G_{max} = \frac{e^2}{h} \frac{\hbar \bar{\Gamma}}{8k_B T} \alpha(T), \quad (1)$$

where $\alpha(T) = \sum_\lambda \alpha_\lambda w_\lambda(T)$ is a weighted sum of normalized lead-dot-lead conductances, $\alpha_\lambda = 2\Gamma_l^\lambda \Gamma_r^\lambda / (\bar{\Gamma}(\Gamma_l^\lambda + \Gamma_r^\lambda))$. The dot is assumed to be symmetrically coupled to the leads, with average tunneling rates $\bar{\Gamma}_l^\lambda = \bar{\Gamma}_r^\lambda = \bar{\Gamma}/2$. In the experimentally relevant regime $(k_B T, \Delta) \ll E_C$, the thermal weights $w_\lambda(T)$ are given by $w_\lambda(T) = 4f(\Delta F_\mathcal{N} - \tilde{E}_F) \langle n_\lambda \rangle_\mathcal{N} [1 - f(E_\lambda - \tilde{E}_F)]$, where $\Delta F_\mathcal{N} = F_\mathcal{N} - F_{\mathcal{N}-1}$ is the difference in the canonical free energy of \mathcal{N} and $\mathcal{N} - 1$ non-interacting electrons on the dot, $\langle n_\lambda \rangle_\mathcal{N}$ is the canonical occupation of level λ with \mathcal{N} electrons on the dot, $\tilde{E}_F = [E_F + e\eta V_g - (\mathcal{N} - 1/2)E_C]$ is the effective Fermi energy with V_g tuned between $\mathcal{N} - 1$ and \mathcal{N} electrons on the dot, E_λ is the energy of level λ , and $f(\epsilon) = 1/(1 + e^{\epsilon/k_B T})$ is the Fermi function. Equation (1) generalizes previous results for low temperatures, $\hbar \bar{\Gamma} \ll k_B T \ll \Delta$, and yields the known distributions for α in that limit [2,3].

Within a noninteracting model, no correlations between neighboring peak heights are expected for $k_B T \ll \Delta$. At higher temperatures, correlations appear as each

level is able to contribute to several nearby peaks. For both numerical RMT data and experimental data, we compute a discrete correlation function $C(n)$ from a sequence of N peaks $(G_{max})_i$

$$C(n) = \frac{1}{N-n} \sum_{i=1}^{N-n} \delta g_i \delta g_{i+n} / \frac{1}{N} \sum_{i=1}^N \delta g_i \delta g_i, \quad (2)$$

where $\delta g_i = ((G_{max})_i - \langle G_{max} \rangle_{N,B})$ is the fluctuation of the i^{th} peak height around the average (calculated over both peak number and magnetic field). The correlation length n_c is then calculated from a Gaussian fit, $C(n) = e^{-(n/n_c)^2}$. The gaussian form is not based on any theoretical model but appears to accurately describe the shape of both the RMT and experimental data.

The quantum dots we discuss are fabricated using e-beam lithography to pattern Cr/Au gates on the surface of a GaAs/AlGaAs heterostructure 900 Å above the 2DEG layer. Multi-gate dot design allows changes in device size and shape by changing gate voltages. Active control of point contact gates during sweeps of the “plunger” gate V_g compensates any unintentional capacitive coupling, allowing many peaks to be swept over without changing the average transmission of the leads. All data were taken using two-wire lock-in techniques with 2 μeV bias at 13 Hz . An electron base temperature of 45 mK and ratio η of gate voltage to dot energy were extracted from the CB peak width versus temperature using standard methods [6]. The charging energy E_C in each configuration was calculated using η and the average peak spacing in gate voltage [7]. The mean level spacing Δ was measured from the sub-structure (corresponding to excited states) in the differential conductance at finite bias using a small ac signal added to a dc bias. Measurements were made with broken time-reversal symmetry, with 3–10 ϕ_o through the device area. For each temperature, V_g was scanned over 50-100 peaks and B was then changed by $\sim \phi_o/A_{dot}$ to give independent peak height statistics.

Figure 1 shows two typical series of CB peaks at lower and higher T , where the increased correlation between peaks at higher T is clearly evident. Peak height fluctuations δg_i (right insets in Fig. 1) are extracted from each series using fits to \cosh^{-2} lineshapes around each peak, and the correlations $C(n)$ are then calculated according to Eq. (2). Plots of $C(n)$ for two dots are shown in Figs. 2(a, b). For both configurations, the correlation length n_c increases with increasing T at lower T . However, for the smaller configuration n_c saturates above 300 mK , while for the larger configuration n_c continues to increase well above this temperature. In still larger devices, saturation is not observed up to temperatures of 700 mK .

Correlation lengths $n_c(T)$ for three measured dot configurations ($\Delta = 20, 28$, and 38 μeV) are shown in Fig. 2(c) along with the RMT results. Each data point in Fig. 2(c) represents data from ~ 500 CB peaks. The

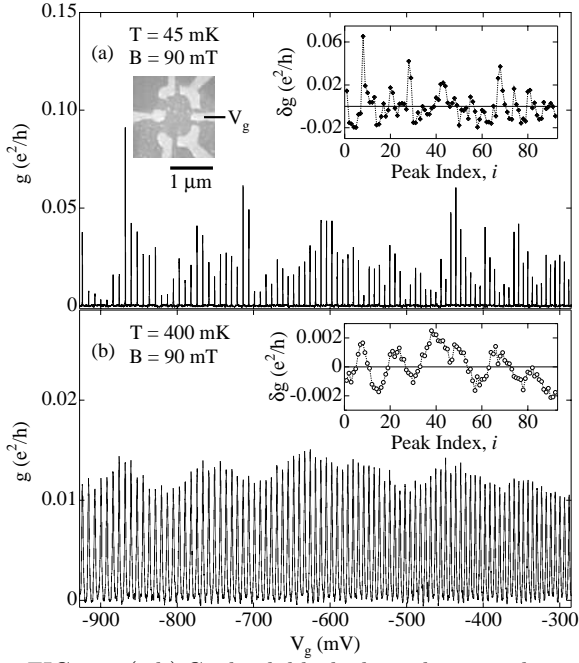


FIG. 1. (a,b) Coulomb blockade peaks in conductance g as a function of gate voltage V_g at (a) 45 mK and (b) 400 mK from device 1. Insets: SEM micrograph of device 1. Peak height fluctuations δg_i extracted from these data sets.

RMT curve was computed by applying Eq. (2) to a peak sequence that is similar in length to the experimental data, and generated according to Eq. (1) assuming a uniformly-spaced spectrum [8]. The RMT results do not change significantly when Wigner-Dyson statistics for the spectrum is included. The saturation of $n_c(T)$ at $m \sim 2$ for $k_B T > 0.5 \Delta$ for the smallest device is evident in Fig. 2(c). The larger dot begins to saturate for larger n , with a larger ratio $k_B T / \Delta$, suggesting that the spectrum of the larger dot is less prone to scrambling. The observed scale of saturation, m , as well as the trend for m to increase with \mathcal{N} , appears consistent with the RPA estimate given above.

As the gate voltage is swept, two distinct changes occur, both of which can cause spectral scrambling. The first is that the number of electrons and size of the dot change; the second is that the shape of the dot changes due to local movement of the boundary at the position of the gate. This second effect was considered recently in Ref. [16] to explain the nearly-Gaussian peak spacing distribution seen in several experiments [11,12,14]. The two effects can be separated using a dot with *two* plunger gates, which allows pure shape distortion without changing \mathcal{N} by increasing one gate voltage and decreasing the other. In practice, it is easier to raster over the two gate voltages, as seen in Fig. 3(a). Horizontal and vertical directions correspond to single-gate CB measurements, while a downward diagonal following a single peak corresponds to pure shape distortion with fixed \mathcal{N} . Correlations in the same dot measured at fixed \mathcal{N} (measured

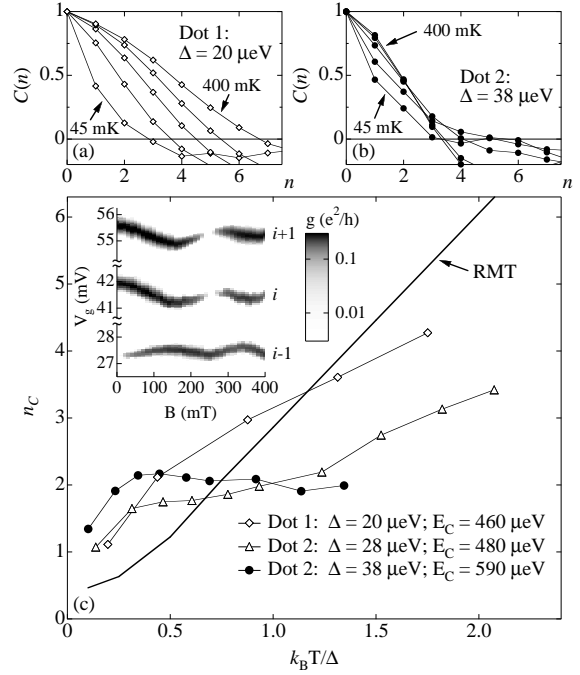


FIG. 2. (a,b) Peak height correlations $C(n)$ at 45 mK, 100 mK, 200 mK, 300 mK and 400 mK for (a) dot 1 and (b) dot 2. (c) Temperature dependence of correlation length n_c for different device configurations, and numerical RMT result. Inset: Grayscale plots of conductance for 3 successive CB peaks, showing paired peaks i and $i+1$, presumably a spin pair.

along diagonals) and changing \mathcal{N} (measured along horizontals) can be compared by evaluating both correlations in terms of V_{g1} rather than n . Comparing $C(\Delta V_{g1})$ for the two cases (Fig. 3(b)) shows that the correlation length associated with shape deformation is larger by a factor of ~ 4 than that associated with a changing \mathcal{N} . This indicates that the saturation of n_c (scrambling) is dominated by changes in electron number rather than by shape distortion. Further work is needed to determine if this result is universally true, but it appears to hold in a variety of gate-confined dots that we have measured.

All dot configurations show an enhanced correlation length $n_c(T)$ at low T compared to RMT, as seen in Fig. 2(c). Thus the data suggest that temperature alone does not explain the enhancement, at least within RMT. Several possible explanations for this have been proposed [15,19,20]; we further note that correlations at low T can result from similar peak heights in spin-paired levels (see Fig. 2(c), inset) which may appear in either adjacent or non-adjacent peaks, depending on the size of interaction-induced spin splitting.

Finally, we investigate the statistics of peak height fluctuations as a function of temperature. It is convenient to consider a normalized distribution to remove any temperature dependence of the average peak height, $\langle \alpha(T) \rangle$. We define $\tilde{\alpha} = \alpha / \langle \alpha \rangle$, so that the distribution $P(\tilde{\alpha})$

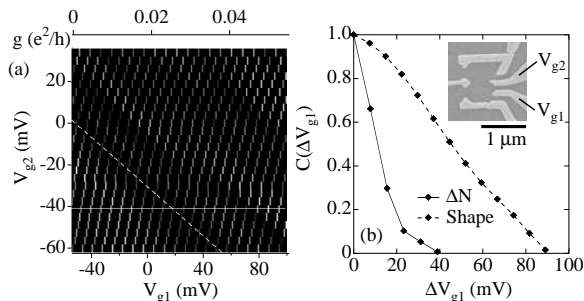


FIG. 3. (a) Grayscale conductance plot of CB peaks as a function of V_{g1} and V_{g2} from device shown in inset of (b), with $\Delta \sim 23 \mu\text{eV}$, at 90 mK. The appearance of peaks as short vertical bars reflects the coarser sampling of V_{g2} compared to V_{g1} ; the patterns of connected bars moving up and to the right are an artifact of this display. (b) Correlation function $C(\Delta V_{g1})$ of peak height fluctuations for fixed \mathcal{N} (dashed curve) and fixed V_{g2} (changing \mathcal{N} , solid curve).

will have $\langle \tilde{\alpha}(T) \rangle = 1$ for all T . The standard deviation $\sigma(\tilde{\alpha}) \equiv \sqrt{\langle \tilde{\alpha}^2 \rangle - 1}$, which characterizes the width of the distribution relative to its mean (i.e., $\sigma(\tilde{\alpha}) = \sigma(\alpha) / \langle \alpha \rangle$), is shown for three dot configurations along with RMT results in Fig. 4. All experimental data show very similar temperature dependences despite significant differences in correlations described above. We conclude that peak height distributions, which are *not* sensitive to scrambling, show more “universal” behavior than correlations. Notice, however, that the experimental data all have smaller height fluctuations than predicted by RMT. This can also be seen in the full distributions $P(\tilde{\alpha})$ comparing experiment (histograms) and RMT (solid lines), shown as insets in Fig. 4. The departure from finite-temperature RMT is likely due to decoherence effects, and might provide a novel tool for measuring decoherence in nearly isolated structures. Ongoing work in this direction is in progress.

We thank A. G. Huibers and S. M. Grossman for contributions to the experiment, and O. Agam, I. Aleiner, B. Altshuler, Y. Gefen, I.V. Lerner, B. Muzykanskii, and M. Stopa for valuable discussions. Work at Stanford supported by the ARO DAAH04-95-1-0221, ONR-YIP N00014-94-1-0622, the NSF-NYI and PECASE programs (Marcus Group); and JSEP DAAH04-94-G-0058 (Harris Group). Work at Yale was supported in part by the DOE DE-FG-0291-ER-40608 and the NSF DMR-9215065.

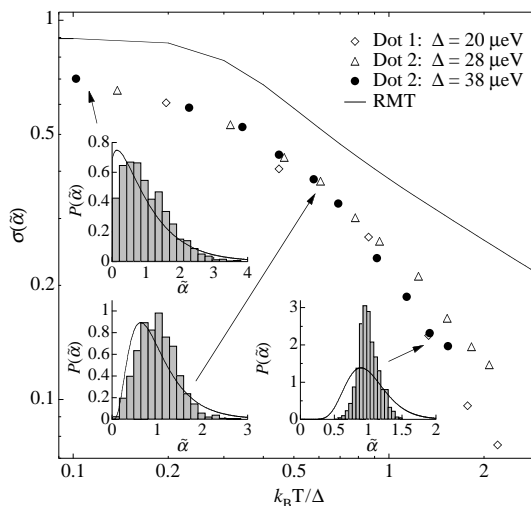


FIG. 4. Temperature dependence of scaled peak height distribution width, $\sigma(\tilde{\alpha})$, along with numerical RMT result (solid curve). Insets: Full distributions of scaled peak heights $P(\tilde{\alpha})$ for all dot configurations combined, at $k_B T = 0.1 \Delta$, $k_B T = 0.5 \Delta$, and $k_B T = 1.5 \Delta$, along with RMT distributions. RMT results use a uniformly-spaced spectrum (rather than Wigner-Dyson).

T. Guhr, A. Muller-Groeling and H. A. Weidenmuller, *Physics Reports* **299**, 190 (1998).

- [2] R. A. Jalabert, A. D. Stone and Y. Alhassid, *Phys. Rev. Lett.* **68**, 3468 (1992).
- [3] V. N. Prigodin, K. B. Efetov and S. Iida, *Phys. Rev. Lett.* **71**, 1230 (1993).
- [4] A. M. Chang, *et al.*, *Phys. Rev. Lett.* **76**, 1695 (1996).
- [5] J. A. Folk, *et al.*, *Phys. Rev. Lett.* **76**, 1699 (1996).
- [6] C. W. J. Beenakker, *Phys. Rev. B* **44**, 1646 (1991).
- [7] L.P. Kouwenhoven *et al.*, in *Mesoscopic Electron Transport*, NATO ASI Series E, vol. 345, edited by L.L. Sohn, L.P. Kouwenhoven and G. Schön (Kluwer, Dordrecht, 1997).
- [8] Y. Alhassid, M. Gökçedağ and A. D. Stone, cond-mat/9807413, *Phys. Rev. B*, in press (1998).
- [9] Y. M. Blanter, A. D. Mirlin and B. A. Muzykanskii, *Phys. Rev. Lett.* **78**, 2449 (1997).
- [10] R. Berkovits and B. L. Altshuler, *Phys. Rev. B* **55**, 5297 (1997).
- [11] U. Sivan, *et al.*, *Phys. Rev. Lett.* **77**, 1123 (1996).
- [12] F. Simmel, T. Heinzel and D. A. Wharam, *Europhys. Lett.* **38**, 123 (1997).
- [13] A. A. Koulikov, F. G. Pikus, B. I. Shklovskii, *Phys. Rev. B* **55**, 9223 (1997).
- [14] S. R. Patel, *et al.*, *Phys. Rev. Lett.* **80**, 4522 (1998).
- [15] M. Stopa, *Semicond. Sci. Technol.* **13**, A55 (1998).
- [16] R. O. Vallejos, C. H. Lewenkopf and E. R. Mucciolo, *Phys. Rev. Lett.* **81**, 677 (1998).
- [17] D. R. Stewart, *et al.*, *Science* **278**, 1784 (1997).
- [18] S. Tarucha, *et al.*, *Phys. Rev. Lett.* **77**, 3613 (1996); L. P. Kouwenhoven *et al.*, *Science* **278**, 1788 (1997).
- [19] G. Hackenbroich, W. D. Heiss and H. A. Weidenmuller, *Phys. Rev. Lett.* **79**, 127 (1997).
- [20] R. Baltin, Y. Gefen, G. Hackenbroich and H. A. Weiden-

[1] For recent articles on mesoscopics and quantum chaos, see: Special issue of *Chaos Solitons and Fractals*, **5**, no. 7/8 (1997); *Quantum Transport and Dissipation*, Ch. 6, T. Dittrich, *et al.* (Wiley-VCH, Weinheim, 1997); C. W. J. Beenakker, *Rev. of Mod. Phys.* **69**, 731 (1997);

muller, cond-mat/9807286.